

# **The Elusive Third Component**

**James F. Meyers  
NASA Langley Research Center  
Hampton, Virginia**

**Symposium on Laser Anemometry  
ASME 1985 Winter Annual Meeting  
November 17-21, 1985  
Miami, Florida**

# The Elusive Third Component

by

James F. Meyers  
Instrument Research Division  
NASA - Langley Research Center  
Hampton, Virginia 23665, USA

## Abstract

The historical development of techniques for measuring three velocity components using laser velocimetry is presented. The techniques are described and their relative merits presented. Many of the approaches currently in use based on the fringe laser velocimeter have yielded inaccurate measurements of turbulence intensity in the on-axis component. A possible explanation for these inaccuracies is presented along with simulation results.

## Nomenclature

$A$	A-component velocity measurement, m/sec
$B$	B-component velocity measurement, m/sec
$f_A$	A-component signal frequency, MHz
$f_B$	B-component signal frequency, MHz
$f_W$	W-component signal frequency, MHz
$U$	U-component velocity measurement, m/sec
$V$	V-component velocity measurement, m/sec
$W$	W-component velocity measurement, m/sec
$\alpha$	Cross beam angle, deg
$\gamma$	Angle between velocity components, deg
$\theta$	Cross beam angle, deg

$\lambda$	Wavelength of laser, m
$\Phi$	Cross beam angle, deg

## **Introduction**

In 1964 Yeh and Cummins from Columbia University first described the use of a laser to measure the velocity of a liquid flow and began a revolution in using non-intrusive techniques to make detailed diagnostic measurements within a flow field. The next year Forman, George and Lewis from Brown Engineering applied the technique to air flows under contract from NASA - Marshall Space Flight Center. The technique utilizes the Doppler effect acting on light scattered from small particles embedded within the flow field that pass through a laser beam. A portion of the Doppler shifted scattered light is collected by a lens system, aligned collinear with the laser beam and focused on the photocathode surface of a photomultiplier. Since the photocathode surface acts as a square law detector, heterodyne mixing of the two light beams yields a signal whose frequency is the Doppler shift frequency which is proportional to the velocity of the scattering particle. In 1969 this concept was expanded directly to a three component system using three appropriately placed photomultipliers by Huffaker, Fuller and Lawrence from NASA - Marshall Space Flight Center. Although this approach had its limitations, it was the first three component laser velocimeter system.

In 1969, Rudd from the British Aircraft Corporation, and separately, Brayton from ARO, Inc. while attempting to simplify the complicated optical approach used by Yeh and Cummins, developed the dual-scatter or fringe type laser velocimeter which yielded greater signal-to-noise ratios than the reference beam configuration. This approach was rapidly expanded by Lennert and Brayton (polarization separation) and Orloff (color separation) to provide two component measurements in 1972. At this point laser velocimeter optical development virtually ceased and the two component laser velocimeter using color separation with Bragg cells used for determining flow directionality became the universally accepted standard. The major exceptions are those efforts by researchers who have searched for the technique to measure the elusive third or on-axis component while maintaining the advantages of the fringe laser velocimeter. The purpose of the present paper is to review these attempts and address the advantages and limitations of the varied approaches.

## **The Beginning**

In the beginning radar technology provided the major source of inspiration for laser velocimetry development during the 1960s. The early researchers reasoned that since light had the same basic properties as radio waves only at a higher frequency, light could be used to measure velocity in the same manner as radar if a coherent, monochromatic light source could be found. With the advent of the continuous wave laser in 1961, the needed light source was available and within three years Yeh and Cummins had developed the first working laser velocimeter, reference 1, and a year later Foreman, George and Lewis used the technique to measure the velocity of an air flow, reference 2. In comparison to radar technology the klystron was replaced with a laser, the antenna with lenses, and the electronic mixer with a photomultiplier.

Scattered light from small particles passing through the laser beam was collected by a lens system and directed collinear with the laser beam (reference) to the photocathode surface of a photomultiplier. Since the photocathode surface is a square law detector, the optical frequency of the reference beam and the Doppler shifted optical frequency from the scattered light are mixed together (heterodyne effect) yielding a signal containing the difference (Doppler) frequency between the two light waves. Using the relations from the Doppler effect, the particle velocity is linearly related to the wavelength of the laser light, the sine of the half angle between the laser beam and the collected scattered light, and the resulting difference (Doppler) frequency.

Continuing with the radar scenario, signals from the photomultiplier were processed using a spectrum analyzer to determine the value of the difference frequency. Later developments continued along these lines with phase lock detectors and frequency lock loops. The major drawback to these signal processors was the requirement of near continuous signals (greater than 15-percent duty cycle). The required particle concentrations are easily obtainable in liquid flows but the difficulty in obtaining these concentrations in air made these techniques unattractive for wind tunnel investigations.

## **Single Component Advances**

During the mid 1960s system development efforts were concentrated on the refinement of the optical system to reduce the collinear wave front tolerance requirements placed on the optical alignment for heterodyning the two light beams at the photocathode surface. In 1967 Goldstein and Kreid, reference 3, developed the concept of dividing the

laser beam into a high power probe beam and a low power reference beam and crossing the two laser beams creating a common volume within the flow field. The photomultiplier was then placed along the reference beam axis providing an alignment aid (the reference beam) since a portion of the scattered light from particles passing through the probe beam at the common volume would be automatically collinear with the reference beam thus removing the problem of wave front alignment at the photomultiplier. Goldstein's approach triggered several other configurations including self-aligning systems by Brayton from ARO, Inc., reference 4, Rudd from the British Aircraft Corporation, reference 5, and Mazumder and Wankum from the University of Arkansas, reference 6. Brayton implemented Goldstein's approach directly using a glass plate to split the input laser beam into the probe and reference beams and crossing them with a single lens. Rudd expanded the input laser beam and used a mask to obtain the two beams and allowed both to impinge on the photomultiplier thus having each beam act as a reference and a probe. Mazumder and Wankum used the opposite approach by masking the collecting lens to form two scattered light beams.

With all the pieces in now place, it was up to Brayton and Goethert in 1970, reference 7, to make the breakthrough which made all other optical configurations obsolete. Brayton and Goethert found that if the two input laser beams were of the same intensity as Rudd had proposed and rotated the collecting optics about the common volume so that neither laser beam reached the photocathode (forming a dual scatter system without the mask as Mazumder and Wankum proposed) that the difference in angle between the two scattered wavefronts was equal at any and all points on the photocathode surface. As shown by Meyers, reference 8, this discovery had the direct effect of increasing the signal-to-noise ratio of the system since a reference beam was not adding shot noise and the receiver optical system could have a collecting solid angle as large as desired limited only by the choice of lens size. This new configuration also reinforced Rudd's proposal that fringes were present within the common volume except now the fringes were real and not virtual. This technique was quickly adopted universally and increased to a two component system by Brayton, Kalb and Crosswy, reference 9, using polarization separation of three input beams and by Grant and Orloff, reference 10, using color separation of two pairs of two beams each using an Argon ion laser. Further research in optical configurations quickly showed that the new technique, now known as the fringe laser velocimeter, was not easily expanded to a three component system and the search for a technique to measure this elusive third component subsided.

### **Third Component Reference Beam**

Early on in 1969 Huffaker, Fuller and Lawrence from NASA - Marshall Space Flight Center, reference 11, extended the technique developed by Yeh and Cummins directly to three components by placing three receiving optical systems symmetrically about the reference beam at 120 degree increments within the plane perpendicular to the laser beam. The three receiving optical systems were placed within a single housing and a tetrahedral prism was used to split the laser beam into three reference beams, one for each photomultiplier. A schematic of the optical system is shown in Figure 1 and a photograph of the system as installed to measure the flow from a supersonic jet is shown in Figure 2. Signal processing was performed by three frequency trackers (frequency lock loop devices). With very heavy particle concentrations within the jet flow, and using conventional instrumentation to process the continuous analog output from the trackers, Huffaker was able to make the first turbulence intensity and turbulence power spectral measurements in three components using a laser velocimeter.

To put this achievement in proper perspective, consider the difficulties that had to be overcome with this complex system: 1) Alignment of a reference beam system requires that the wave fronts from the reference beam and the collected scattered light be parallel to within 0.0015 degrees for heterodyning to take place on the photocathode surface; 2) The signal-to-noise of a reference beam system is extremely low due to the small collecting solid angle (only collected scattered light common with the reference beam will heterodyne) and the relatively high ratio between the reference beam power and the scattered light power yielding a large shot noise contribution; 3) Concentrations of  $7 \times 10^6$  particles per cubic centimeter are required to yield the duty cycle necessary for the signal processors, reference 12; and, 4) the errors involved in the coordinate transformation of a non-orthogonal coordinate system to an orthogonal system where components containing a large velocity contributions from the directed flow are combined to obtain the very small  $V$  and  $W$  contributions. A further problem, later rectified by the inclusion of an optical single side band modulator in the reference beam, reference 13, was direction ambiguity in the velocity measurements.

In 1973 Orloff and Logan, reference 14, combined the new fringe laser velocimeter technology with a coaxial reference system to obtain three component measurements. A schematic showing the system is presented in Figure 3 along with their approach for increasing the signal-to-noise ratio. (The signal is obtained by subtracting the output from two photomultipliers, each viewing a fringe pattern displaced from the other by half a fringe spacing, to enhance the coherent part (signal

frequency) while removing the random part (shot noise)). Although this system seems straight forward and works quite well in the laboratory, there are three problem areas which must be considered. First the reference beam system has a very long measurement volume (defined by the limits of the wave front curvature typically 10 percent of the focal length) unless coincidence between the measurements (all three components must obtain a velocity measurement from the same particle) is imposed. Secondly, the Doppler shift of scattered light in direct backscatter is twice the component velocity divided by the laser wavelength which places an upper limit of about 25 m/sec in the  $W$  component for a 100 MHz signal processor limit. The third and most troublesome area is sensitivity of the system to vibration of the tunnel window, and the tunnel wall or model where the probe beam terminates. The amount of scattered light is sufficient from these surfaces, even though they are usually far from the sample volume, to mask the signal from particles. Therefore, this approach appears to be limited to measurements of flow fields within open jets.

### **Third Component Fringe**

In 1980 Orloff and Olson, reference 15, used two standard configuration single component fringe laser velocimeters angled symmetrically about the  $W$  component axis with a separation angle of 25 degrees (Figure 4). Coincident signals from the two laser velocimeter components were processed by high-speed burst counters and converted to the  $U$  and  $W$  velocity components for each particle during data processing in the acquisition computer system.

This approach was modified by Yanta and Aushermann (reference 16, illustrated in Figures 5 and 6) in 1981 by rotating the optical system such that the  $U$ -component of velocity was measured directly (allowing the inclusion of a second standard component of optics to measure the  $V$ -component). *The remaining component,  $A$* , was a single component system rotated 22.8 degrees about the sample volume and measured particle velocities containing contributions from  $U$  and  $W$ . The signals from each of the three components were segregated by using three laser wavelengths with the cross beam angle of the  $A$ -component adjusted to yield the same signal frequency as the  $U$ -component for a particle passing along the  $U$  direction. Signals from the  $U$ -component were combined with signals from the  $A$ -component in an electronic double balanced mixer yielding the sum and difference frequencies between the two signals. The difference frequency (represented by the numerator in the equation in Figure 6) is signal due to the contribution of  $W$  in the  $A$ -component measurement. A trigonometric adjustment of the difference frequency yields the  $W$ -component measurement. This

system was the first three component laser velocimeter using only the fringe technique.

In 1982 Meyers and Wilkinson, reference 17, used the direct approach by placing a standard single component optical system overhead and measuring the third component directly, (Figure 7). The signals from the three components were segregated using three wavelengths from an Argon ion laser. The major advantage of this configuration is the direct measurement of the  $W$ -component. Another advantage is if a coincident measurement requirement is imposed, the measurement volume becomes a sphere with a diameter equal to the beam waist allowing highly detailed investigations within flow fields with large gradients. However this approach requires optical systems to be placed on at least two adjacent sides of the facility and is thus not practical for large facility applications.

A unique configuration of five laser beams was used by Schock, Regan, Rice and Chlebeck, reference 18, in 1983 to measure three components of velocity in the flow above a piston and by Meyers and Hepner, reference 19, in 1984 to measure the flow within a juncture. Two beams of one color (blue) were used to measure the standard  $V$  component and the remaining three of a second color (green) to form three fringe patterns in the  $U$ - $W$  plane (Figures 8 and 9). The three signals from the fringe patterns formed by the green beams were separated using two Bragg cells to generate three different bias frequencies allowing frequency separation. These signals were passed through the electronics network illustrated in Figure 10 to obtain the  $U$ -component directly from the two outside beams and the  $W$ -component by mixing the signals from the remaining fringe patterns to obtain the difference frequency.

As can be seen, these approaches are similar and have fixed focal distances. In large wind tunnel applications, optical scanning is necessary due to the distances traveled making these techniques unattractive. A possible solution is another variation combining the technique used by Yanta and the five beam system, (Figure 11). In this configuration a standard two component system is used to measure the  $U$  and  $V$ -components and a single beam is brought to the sample volume from a relatively large angle which forms three fringe patterns in the manner of the five beam system. However, like Yanta's approach the fringe pattern of interest is the  $A$ -component (Figure 12) as defined by the center beam and the single beam. The thought is that a single beam is easier to control via a small single mirror to keep it within in the sample volume as the standard system is zoomed. Focal length of the single beam is also not as critical as a full component because fringes will be formed within the sample volume regardless of the location of the

beam waist, whereas coincident measurements could not even be made if the focal length of the full component was in error.

### **There Still Must Be a Problem**

With so many configurations it would seem that the correct approach is still eluding researchers. In general this is true, however upon closer examination of the fringe type configurations one finds that they are mathematically equivalent. Each approach utilizes a component angled about the sample volume to obtain a measure of a portion of the  $W$ -component velocity with the overhead configuration being the limit. With the exception of the overhead configuration, these approaches yield few widely spaced fringes along the  $W$ -component. This accentuates any random measurement errors by the signal processor (typically negligible in the normal  $U$  and  $V$ -component measurements) resulting in an artificially large measure of standard deviation in the  $W$ -component.

The similarity of these systems may be seen by comparing the conversion equations given in the figures. Each conversion is a subtraction of the two common component measurements (with the proper trigonometric adjustments) divided by the sine of the angle between the optical axis of the two components. (The overhead configuration has an angle between the two components of 90 degrees making the denominator equal to unity and removing the contribution of the second component because it is multiplied by the cosine of 90 degrees). This sine term becomes the critical element in determining the accuracy of the  $W$ -component measurement. For example consider the equation for the five beam system:

$$W = \frac{B - A}{2 \sin \frac{\theta}{2}} \quad (1)$$

$$f_W = \frac{\lambda}{2 \sin \frac{\theta}{2}} \frac{f_B - f_A}{2 \sin \frac{\theta}{2}} \quad (2)$$

As the angle between the two components ( $\theta$ ) is reduced, the value of signal frequency for a given  $W$ -component velocity is reduced inversely proportional to the sine of that angle. That is if  $\theta$  is 30 degrees, 1 m/sec

in  $W$  would yield an effective frequency difference of 0.521 MHz whereas if  $\theta$  is 10 degrees the frequency difference reduces to 0.0591 MHz. Therefore if the constraints of the measurement require  $\theta$  to be small, random errors in the measurement frequency due to signal-to-noise, mixer noise, quantizing, etc. will yield an increase in the measurement of standard deviation even to the point of totally masking the measurement of turbulence intensity.

A measure of these random errors may be obtained by simulating the signal burst generation and processing with a high-speed burst counter. An ideal signal with a visibility of unity was generated on a computer, integrated and used as the control for a Poisson random number generator to yield a simulation of the photon resolved signal reaching the photomultiplier using the technique described in reference 20. Signals at various frequencies from 5 MHz to 50 MHz were simulated containing from 150 photons to 2500 photons with a fringe count of 20 within the  $1/e^2$  limits of the fringe pattern. These signals were convolved with the photomultiplier response (250 MHz) to yield a simulation of the signal available from the photomultiplier. This signal was then input to a model of a high-speed burst counter with double threshold detection circuits using zero crossing triggers and a 5:8 count comparison signal check. A sample of 100 signal bursts, each burst containing the same signal frequency, was used in the simulation with the starting phase of each burst controlled by a uniform random number generator to simulate the random passage of the particles through different points within the sample volume. The standard deviation of the measured frequencies of the ensemble of signal bursts accepted within the 2 percent 5:8 comparison of the counter was calculated yielding a measure of the effect of signal-to-noise and counter quantizing error on the measurement.

The results of this study are presented in Figure 13 with the standard deviations plotted as a function of photon count for signal frequencies of 6.25 MHz, 12.5 MHz and 25.0 MHz. As expected the lower the number of photons and/or greater bandwidth, the greater the measured standard deviation. For example, the effect of photon count may be illustrated by considering the case where the signal frequency is 6.25 MHz and the photon count is adjusted from 618 to 1233 to 2465 photons per burst. This results in standard deviations of 0.048 MHz, 0.041 MHz and 0.025 MHz, respectively. If the photon count is kept constant, e.g., 617 photons per burst, and the signal frequencies adjusted from 25 MHz, 12.5 MHz and 6.25 MHz (bandwidths of 16, 8, and 4 MHz respectively), the effect of bandwidth is illustrated with the resulting measurements of standard deviation of 0.1669 MHz, 0.0984 MHz and 0.0480 MHz, respectively. The effect of this increase in standard deviation on the velocity measurements as a function of the angle

between the two components is illustrated along with quantizing error as a reference in the following table:

Table 1. - Dependence of Standard Deviation on Configuration

<b>Yanta's Configuration</b>	<b>25 MHz</b>	<b>12.5 MHz</b>	<b>6.25 MHz</b>
<b>U-component (<math>\theta = 4^\circ</math>)</b>			
Mean (m/sec)	184.28	92.14	46.07
Standard Deviation (m/sec)	1.23	0.73	0.35
Turbulence Intensity (%)	0.67	0.79	0.76
Quantizing Error (%)	0.36	0.18	0.09
<b>W-component (<math>\gamma = 30^\circ</math>)</b>			
Standard Deviation (m/sec)	2.20	1.30	0.63
Turbulence Intensity (%)	1.19	1.41	1.37
Quantizing Error (%)	0.36	0.18	0.09
<b>W-component (<math>\gamma = 10^\circ</math>)</b>			
Standard Deviation (m/sec)	5.09	3.00	1.46
Turbulence Intensity (%)	2.76	3.26	3.17
Quantizing Error (%)	0.36	0.18	0.09
<b>Five Beam Configuration</b>			
<b>U-component (<math>\theta = 15^\circ</math>)</b>			
Mean (m/sec)	24.85	12.42	6.21
Standard Deviation (m/sec)	0.17	0.10	0.05
Turbulence Intensity (%)	0.67	0.79	0.77
Quantizing Error (%)	0.36	0.18	0.09
<b>W-component (<math>\theta = 15^\circ</math>)</b>			
Standard Deviation (m/sec)	1.26	0.74	0.36
Turbulence Intensity (%)	5.07	5.96	5.80
Quantizing Error (%)	0.36	0.18	0.09

**25 MHz    12.5 MHz    6.25 MHz**

*U*-component ( $\theta = 10^\circ$ )

Mean (m/sec)	73.79	36.90	18.45
Standard Deviation (m/sec)	0.49	0.29	0.14
Turbulence Intensity (%)	0.66	0.79	0.76
Quantizing Error (%)	0.36	0.18	0.09

*W*-component ( $\theta = 5^\circ$ )

Standard Deviation (m/sec)	11.28	6.65	3.24
Turbulence Intensity (%)	15.29	18.02	17.56
Quantizing Error (%)	0.36	0.18	0.09

Therefore large angles are required between the two components to reduce the apparent increase in turbulence intensity but even large angles may not be sufficient. Increasing signal strength (i.e., increasing photon count per burst) and thus signal-to-noise ratio either by increasing laser power or increasing collecting solid angle will reduce the apparent turbulence intensity further, e.g., an increase of a factor of four will reduce the standard deviation by a factor of two for the 6.25 MHz case.

A generalized relationship may be obtained from these results if the standard deviation is divided by the filter bandwidth and plotted versus amplitude divided by the signal frequency. The curve presented in Figure 14 was obtained via least squares fit of the simulation results and found to have the form:

$$\frac{\textit{standard deviation}}{\textit{bandwidth}} = 0.0029 \frac{\textit{amplitude}}{\textit{frequency}}^{0.34} \quad (3)$$

In practice the laser velocimeter components will contain Bragg cells to determine directionality thus increasing the signal frequency obtained from the photomultiplier. Typically this frequency is reduced through electronic mixers with either a signal from an oscillator or a signal from the second component acting as the reference. These two procedures were also simulated and yielded the following equations:

Mixer with cw reference

$$\frac{\textit{standard deviation}}{\textit{bandwidth}} = 0.0030 \frac{\textit{amplitude}}{\textit{frequency}}^{0.28} \quad (4)$$

## Mixer with second component as reference

$$\frac{\text{standard deviation}}{\text{bandwidth}} = 0.0057 \frac{\text{amplitude}}{\text{frequency}}^{0.25} \quad (5)$$

The results are presented along with the non-mixed example in Figure 15. The results from mixing with a signal from an oscillator has the same standard deviation as the non-mixed example and even a lower level when the oscillator output is at a higher level (0.4 V peak-to-peak in the simulation) than the photomultiplier output. It was also found that the standard deviation was approximately 1.8 times larger when the signals from two components were mixed together. Based on these results, one would expect that measuring the two components separately would be superior. However when the component measurements are subtracted to yield the  $W$ -component measurement, the resultant standard deviation will be a multiplication of the individual standard deviations yielding the same results as when the two signals are mixed together.

In practice this increase in standard deviation due to signal-to-noise has rendered the measurement of turbulence intensity in the  $W$ -component useless. During the experiments conducted in reference 19, the turbulence intensity measurements in the  $W$  component were found to be approximately three times larger than the  $U$  component measurements and 10 times larger than the  $V$ -component measurements. Several researchers (private communication) using other optical configurations have indicated similar results.

One would expect that increasing the signal-to-noise ratio would solve this problem. The most straight forward approach to increasing signal-to-noise is increasing the number of photons arriving at the photocathode surface. Unfortunately the signal levels obtained during the tests in reference 19 was approximately half the value of the saturation voltage of the photomultiplier, therefore this approach is not sufficient. A possible aid would be Orloff's approach, reference 14, of combining the signals from two photomultipliers, each viewing a fringe pattern half a fringe spacing apart. This technique has the advantage of doubling the signal level while decreasing the random shot noise yielding a large increase in signal-to-noise ratio. A second possibility is the development of a new type signal processor which is less sensitive to noise than the high-speed burst counter (but that is another story *the elusive perfect signal processor*).

## Concluding Remarks

Attempts by several researchers to find the elusive third component have been presented. All of these configurations contain limitations in either optical constraints or inaccuracies in the measure of the standard deviation of the *W* component measurement. The overhead view yields the most accurate measurement, however the configuration requires optical access from two adjacent sides of the measurement area which makes the technique unattractive for large wind tunnels. The remaining configurations, each containing optical limitations especially scanning the long distances required in large wind tunnels, also suffer from inaccurate measurements of turbulence intensity due to the limitations of signal-to-noise. Therefore the *W*-component remains the elusive third component.

## References

1. Yeh, Y.; and Cummins, H. Z.: *Localized Fluid Flow Measurements with an He-Ne Laser Spectrometer*, Applied Physics Letters, Vol. 4, pp. 176-178, May 1964.
2. Foreman, J. W.; George, E. W.; and Lewis, R. D.: *Measurement of Localized Flow Velocities in Gases with a Laser Doppler Flowmeter*, Applied Physics Letters, Vol. 7, No. 4, August 1965.
3. Goldstein, R. J.; and Kreid, D. K.: *Measurement of Laminar Flow Developed in a Square Duct Using a Laser Doppler Flowmeter*, Journal of Applied Mechanics, Item 34, Series E, No. 4, pp. 813-818, December 1967.
4. Brayton, D. B.: *A Simple Laser, Doppler Shift, Velocity Meter with Self-Aligning Optics*, Presented at the Electro-Optical Systems Design Conference, September 16-18, 1969, New York, NY.
5. Rudd, M. J.: *A Self Aligning Laser Doppler Velocimeter, ICO-8, Optical Instruments and Techniques*, Oriel Press, 58-166, 1969.
6. Mazamder, M. K.; and Wankum, D. L.: *Signal to Noise Ratio and Spectral Broadening in Turbulence Structure Measurement using a C.W. Laser*, Applied Optics, Vol. 9, No. 3, 633, 1970.
7. Brayton, D. B.; and Goethert, W. H.: *A New Dual Scatter, Laser, Doppler Shift Velocity Measuring Technique*, Instrumentation in the Aerospace Industry, Vol. 16, pp. 14-26, 1970.

8. Meyers, J. F.: *Investigation of Basic Parameters for the Application of a Laser Doppler Velocimeter*, AIAA 6th Aerodynamic Testing Conference, Paper 71-288, March 1971.
9. Brayton, D. B.; Kalb, H. T.; and Crosswy, F. L.: *A Two-Component, Dual-Scatter Laser Doppler Velocimeter with Frequency Burst Signal Readout*, Presented at the Project Squid Workshop on The Use of the Laser Doppler Velocimeter for Flow Measurements, Purdue University, March 9-10, 1972.
10. Grant, G. R.; and Orloff, K. L.: *Two-Color Dual-Beam Backscatter Laser Doppler Velocimeter*, Applied Optics, Vol. 12, No. 12, pp. 2913-2916, December 1973.
11. Huffaker, R. M.; Fuller, C. E.; and Lawrence, T. R.: *Application of Laser Doppler Velocity Instrumentation to the Measurement of Jet Turbulence*, International Automotive Engineering Congress, Detroit, MI, January 13-17, 1969.
12. Fridman, J. D.; Kinnard, K. F.; and Meister, K.: *Laser Doppler Instrumentation for the Measurement of Turbulence in Gas and Fluid Flows*, Electro-Optical Systems Design Conference, New York, NY, September 16-18, 1969.
13. Huffaker, R. M.: *Laser Doppler Detection Systems for Gas Velocity Measurement*, Applied Optics, Vol. 9, No. 5, pp. 1026-1039, May 1970.
14. Orloff, K. L.; and Logan, S. E.: *Confocal Backscatter Laser Velocimeter with On-Axis Sensitivity*, Applied Optics, Vol. 12, No. 10, pp. 2477-2481, October 1973.
15. Orloff, K. L.; and Olsen, L. E.: *High-Resolution LDA Measurements of Reynolds Stress in Boundary Layers and Wakes*, AIAA Paper 80-0436, 1980.
16. Yanta, W. J.; and Ausherman, D. W.: *A 3-D Laser Doppler Velocimeter for use in High-Speed Flows*, Seventh Biennial Symposium on Turbulence, University of Missouri-Rolla, September 21-23, 1981.
17. Meyers, J. F.; and Wilkinson, S. P.: *A Comparison of Turbulence Intensity Measurements using a Laser Velocimeter and a Hot Wire in a Low Speed Jet Flow*, Presented at the International Symposium on Applications of Laser-Doppler Anemometry to Fluid Mechanics, Lisbon, Portugal, July 5-7, 1982.

18. Schock, H. J.; Regan, C. A.; Rice, W. J.; and Chlebeck, R. A.: *Multicomponent Velocity Measurement in a Piston-Cylinder Configuration Using Laser Velocimetry*, TSI-Quarterly, Vol. 9, Issue 4, Oct-Dec 1983.
19. Meyers, J. F.; and Hepner, T. E.: *Velocity Vector Analysis in a Junction Flow Using a Three Component Laser Velocimeter*, Presented at the Second International Symposium on Applications of Laser Anemometry to Fluid Mechanics, Lisbon, Portugal, July 2-4, 1984.
20. Mayo, W. T., Jr.: *Modeling Laser Velocimeter Signals as Triply Stochastic Poisson Processes*, Presented at the Minnesota Symposium on Laser Anemometry, Bloomington, MN, October 22-24, 1975.

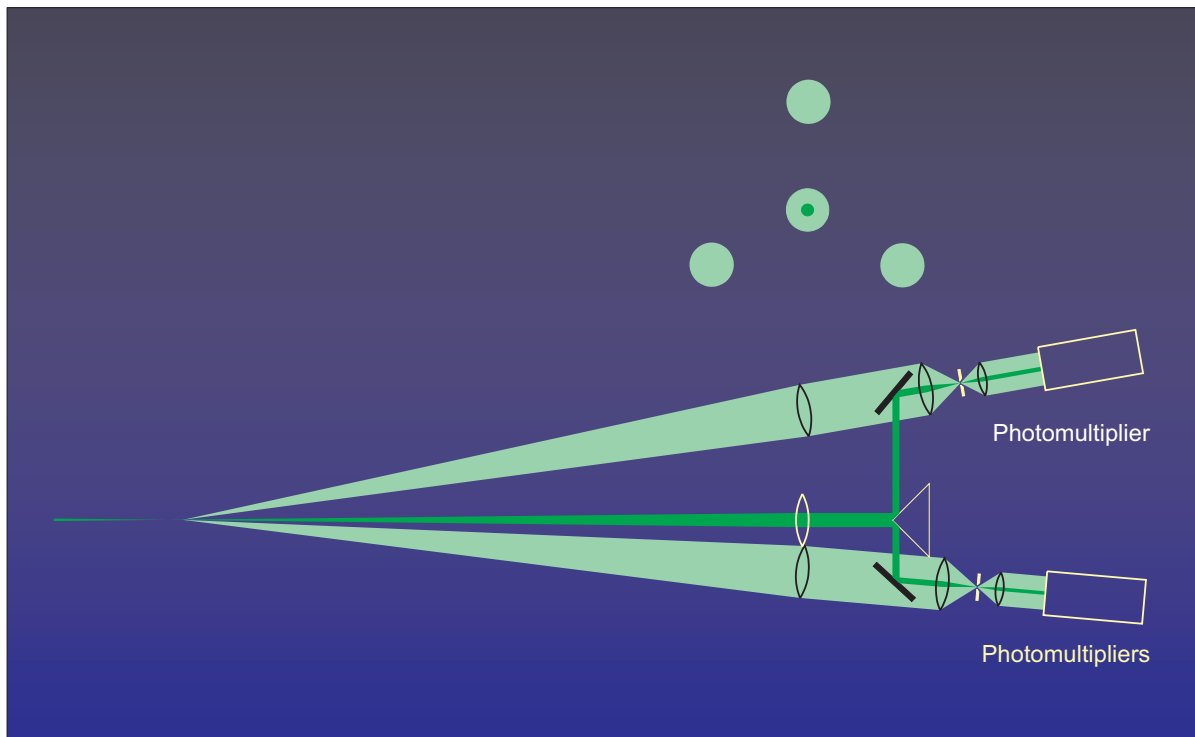


Figure 1. Diagram of the three component reference beam system developed by Huffaker, Fuller, and Lawrence.

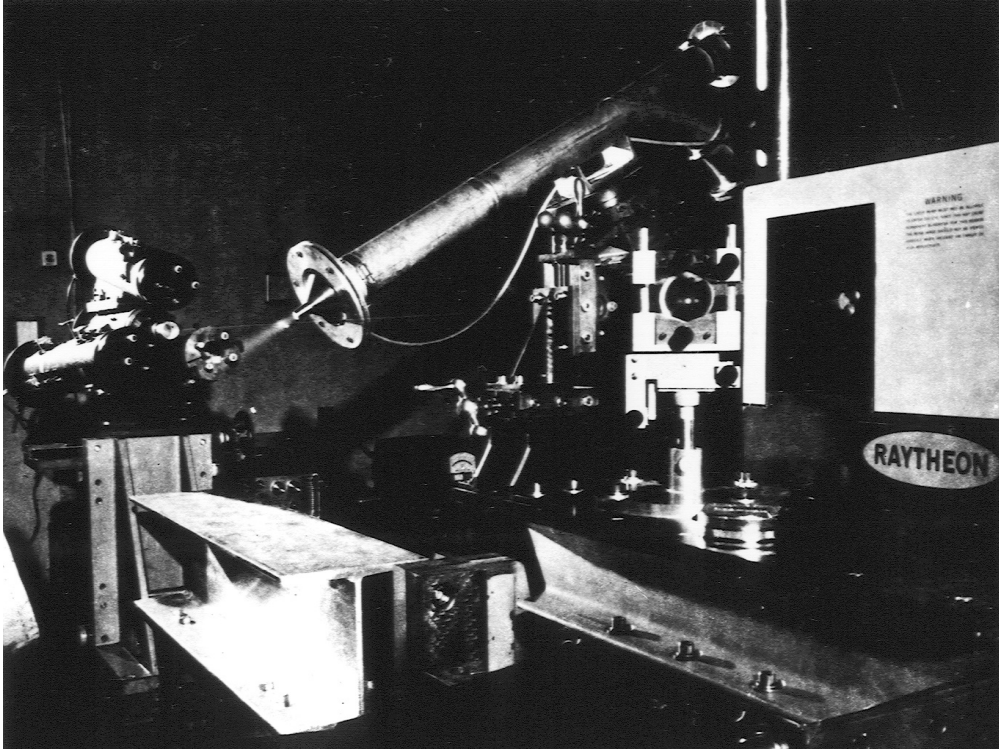


Figure 2. Installation of the three component reference beam system to measure a supersonic jet.

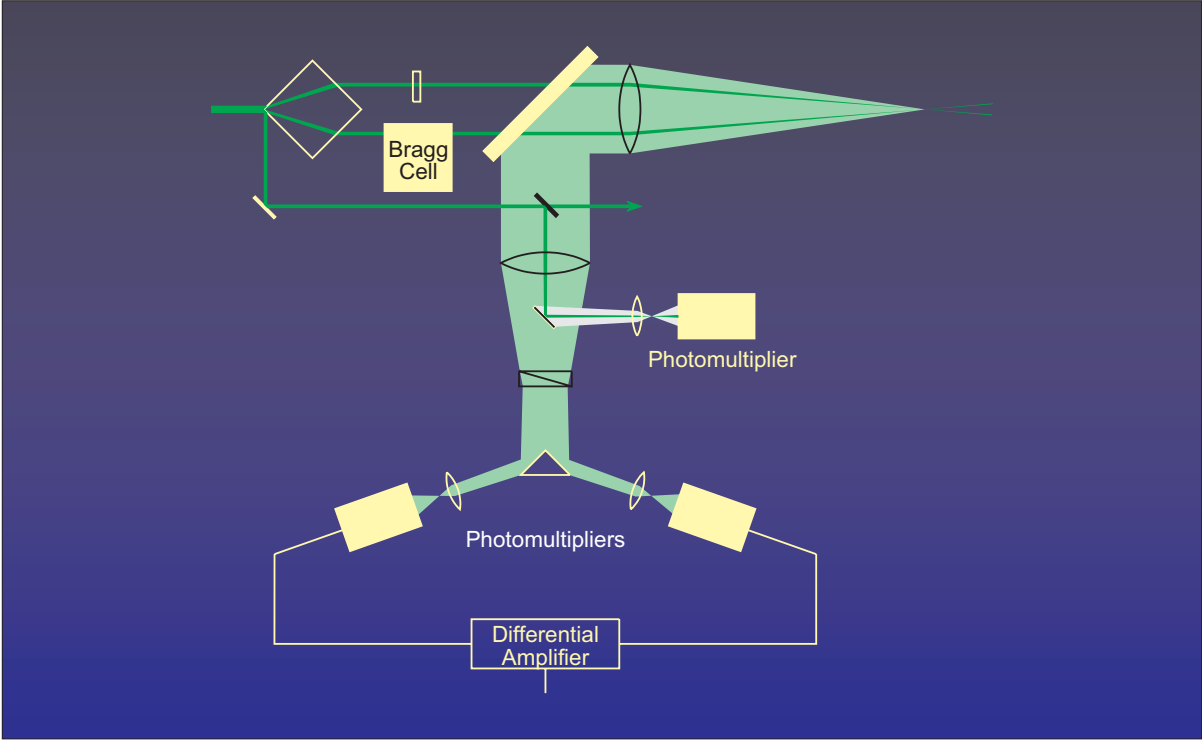


Figure 3. Diagram of the on-axis reference beam system combined with a single fringe component developed by Orloff and Logan.

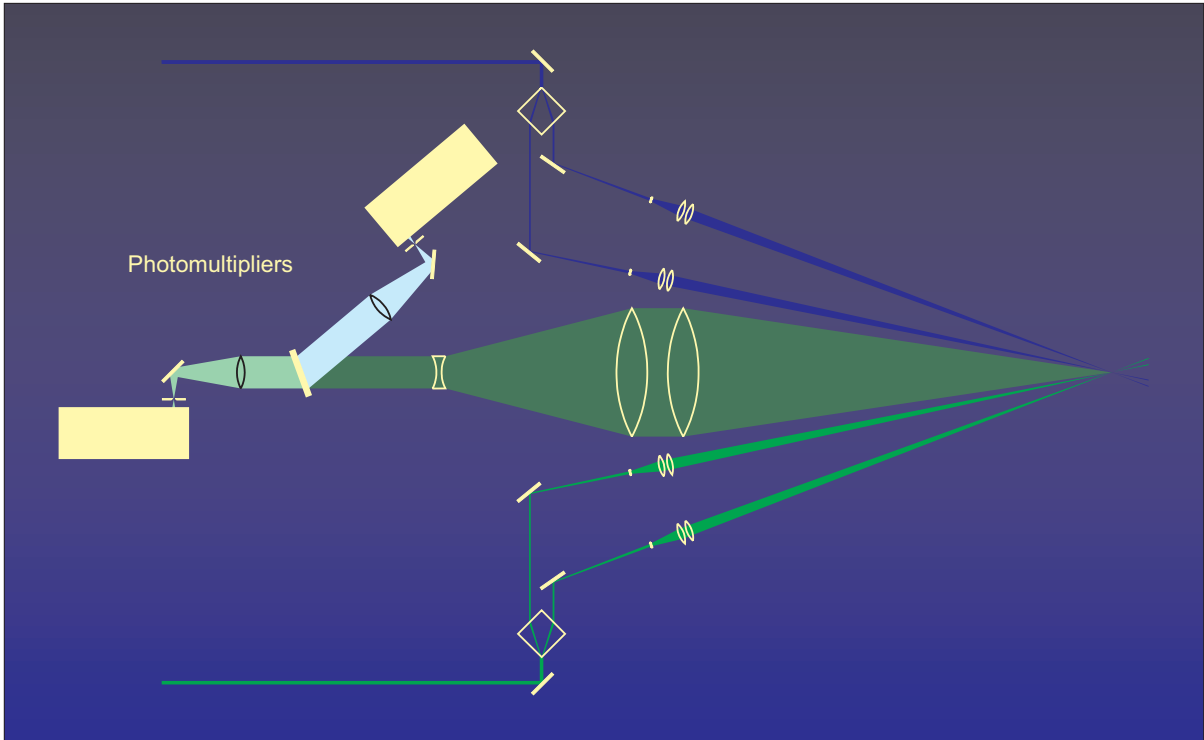


Figure 4. Diagram of the symmetric crossed fringe systems developed by Orloff and Olsen.

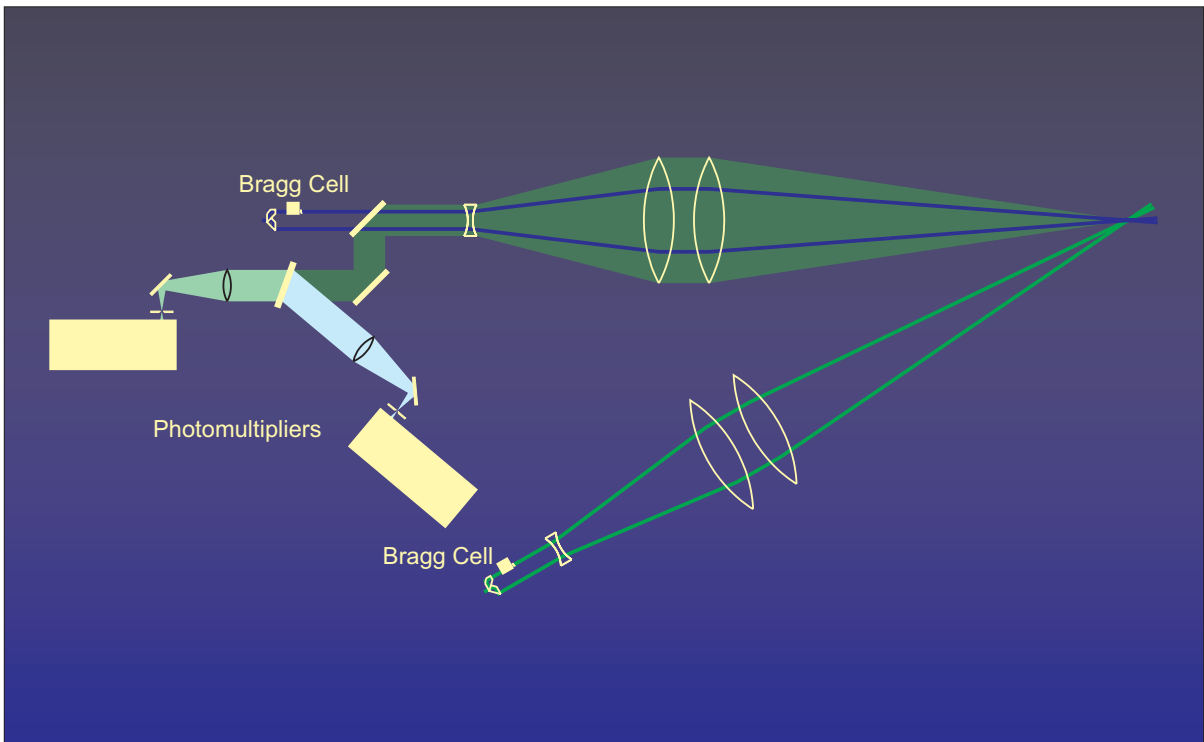


Figure 5. Diagram of the off-axis crossed fringe systems developed by Yanta and Ausherman.

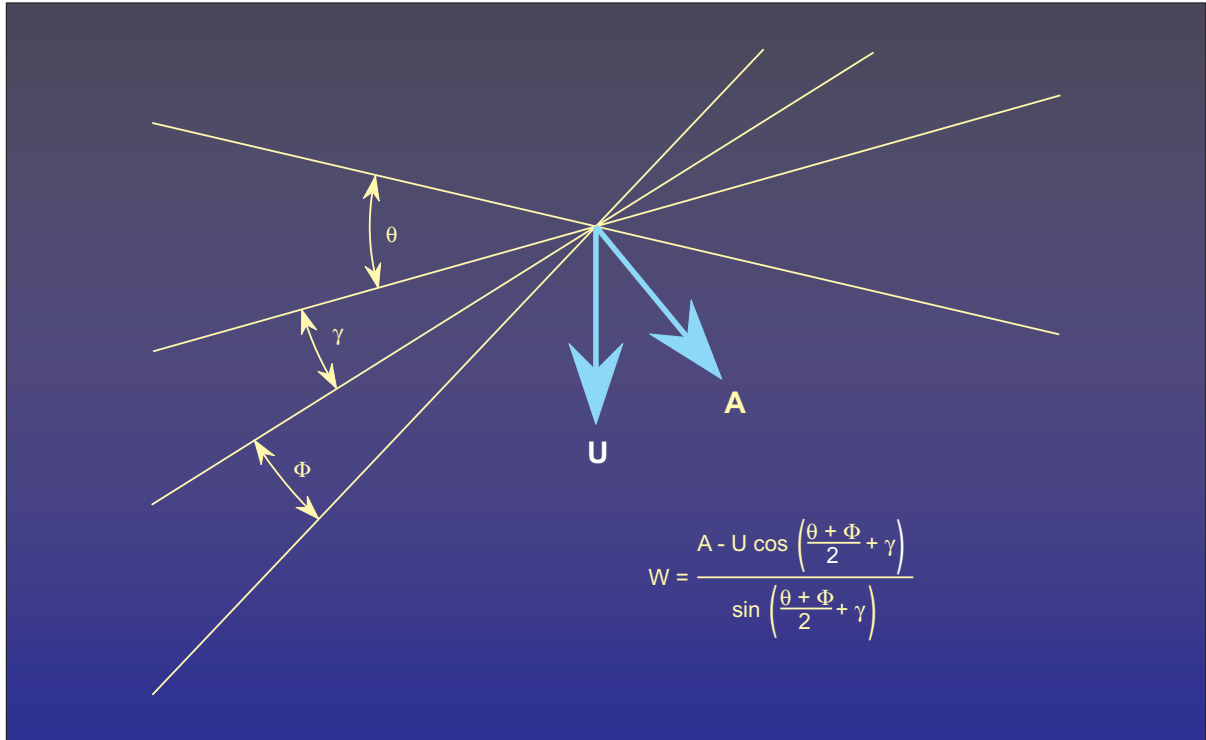


Figure 6. Component orientation of the off-axis crossed fringe system.

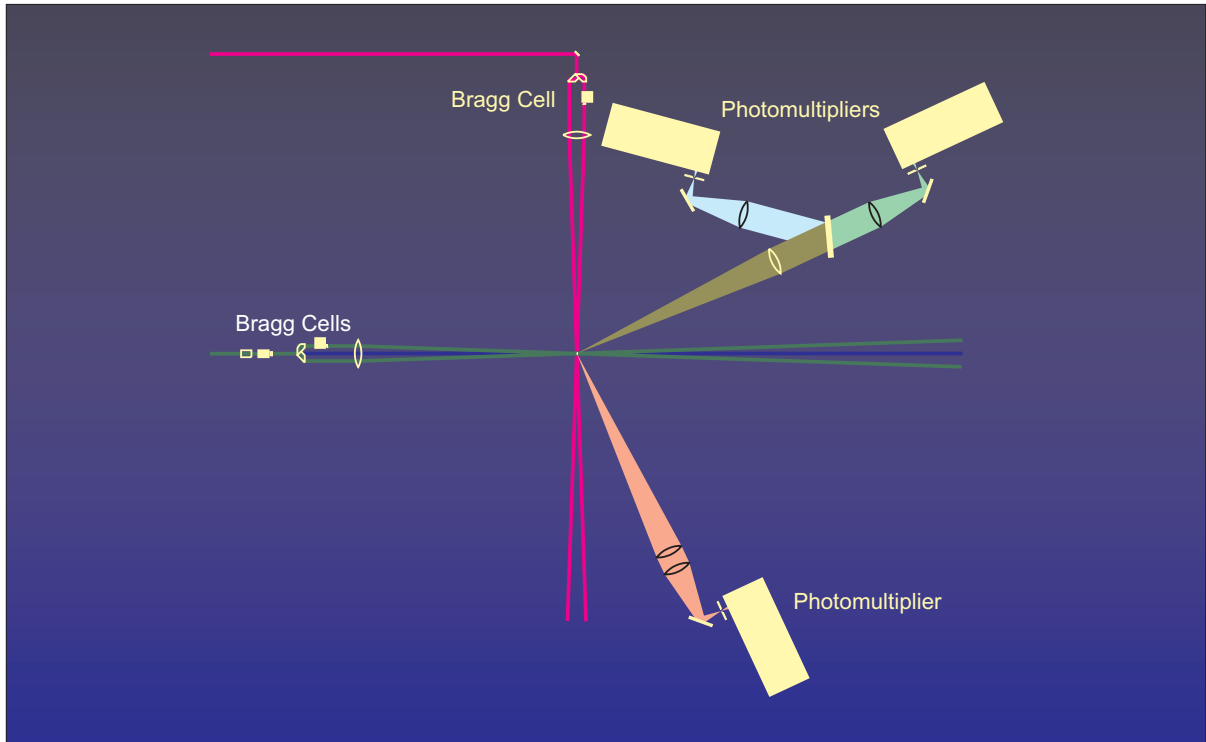


Figure 7. Diagram of the orthogonal crossed fringe system developed by Meyers and Wilkinson.

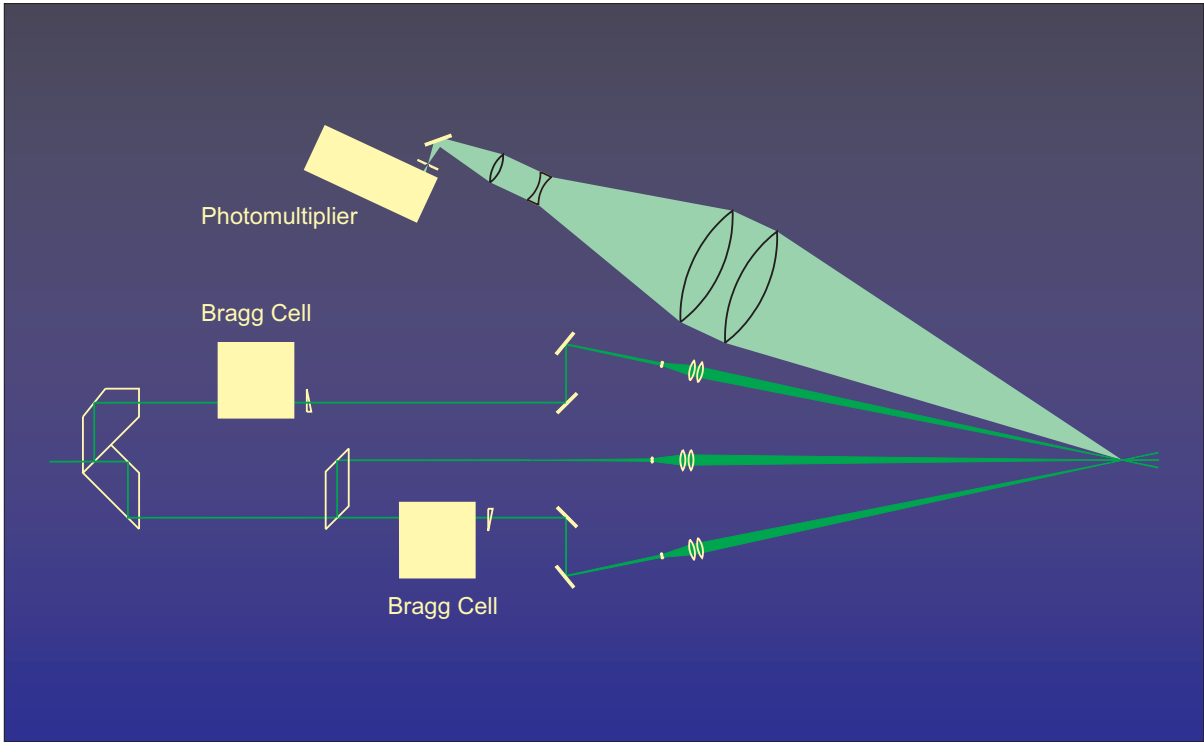


Figure 8. Diagram of the five beam, three component laser velocimeter.

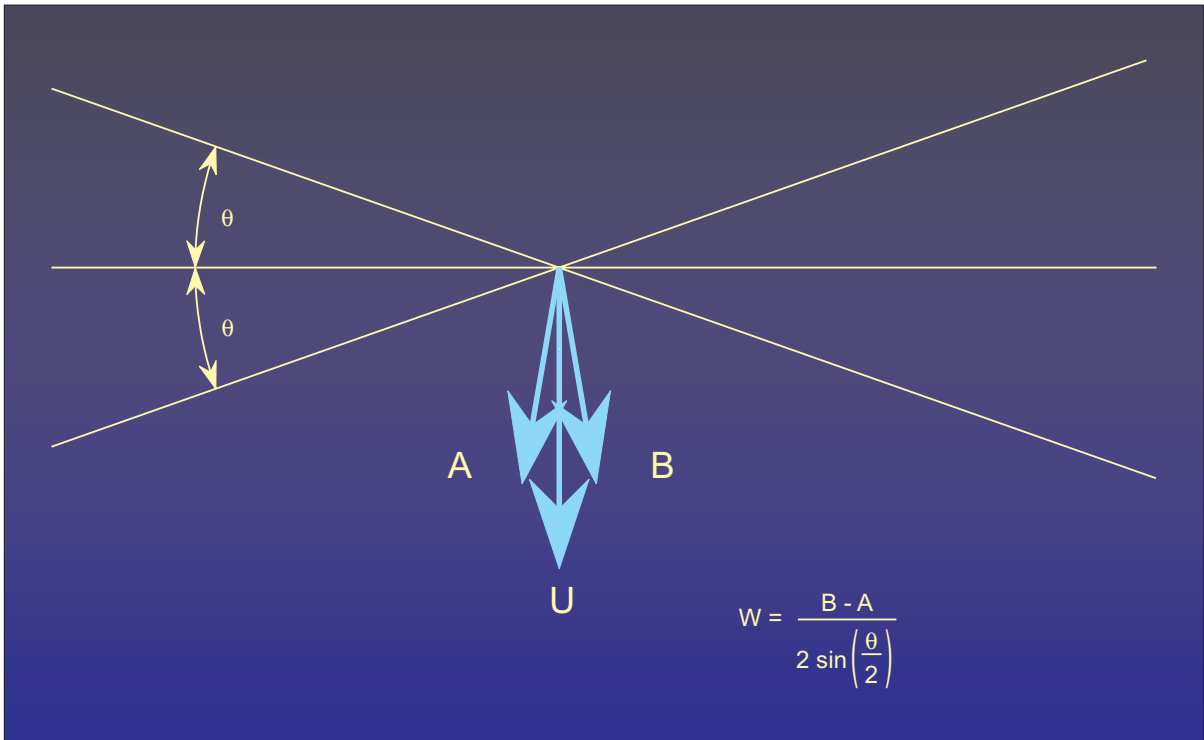


Figure 9. Component orientation of the five beam, three component laser velocimeter.

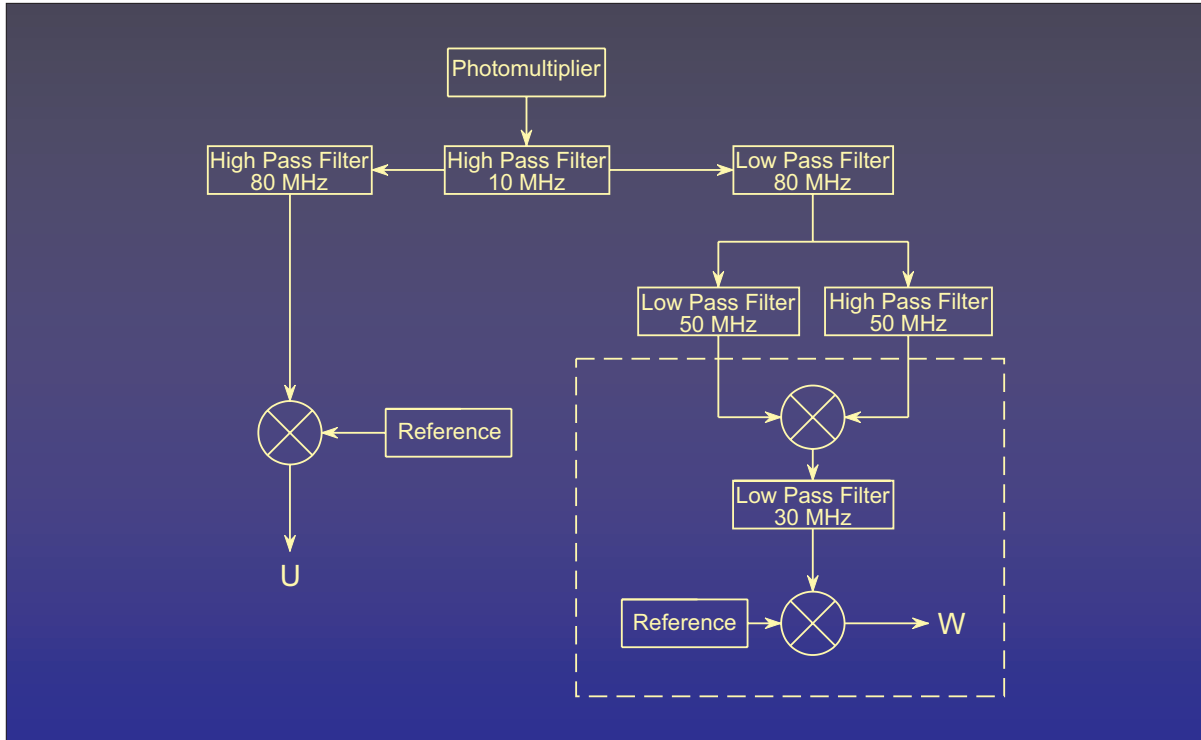


Figure 10. Block diagram of the signal conditioning electronics for the five beam, three component laser velocimeter.

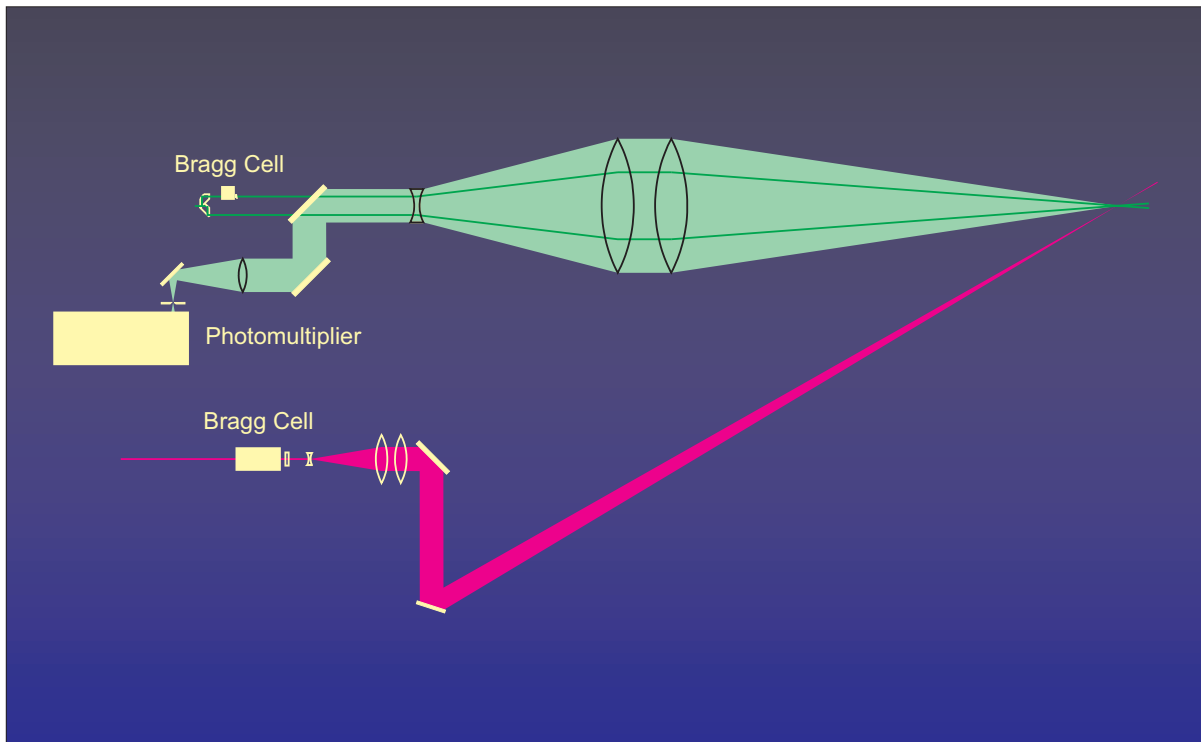


Figure 11. Diagram of a proposed off-axis single beam, three component laser velocimeter.

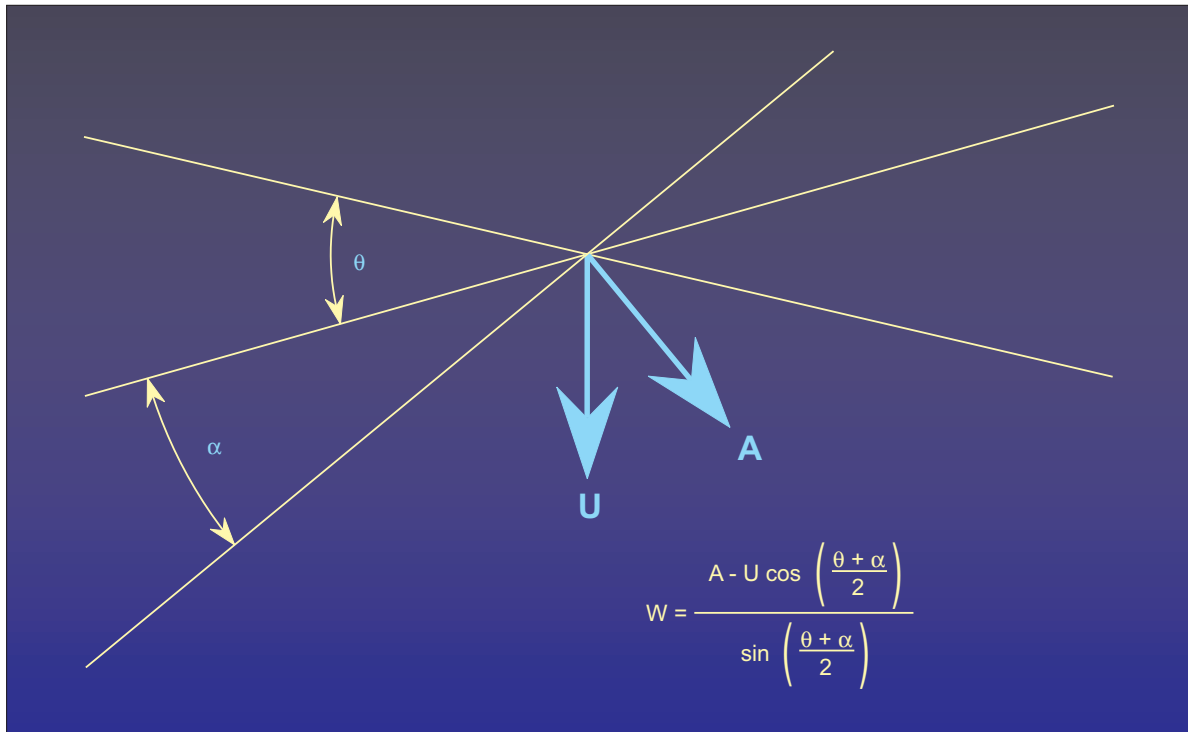


Figure 12. Component orientation of the off-axis single beam, three component laser velocimeter.

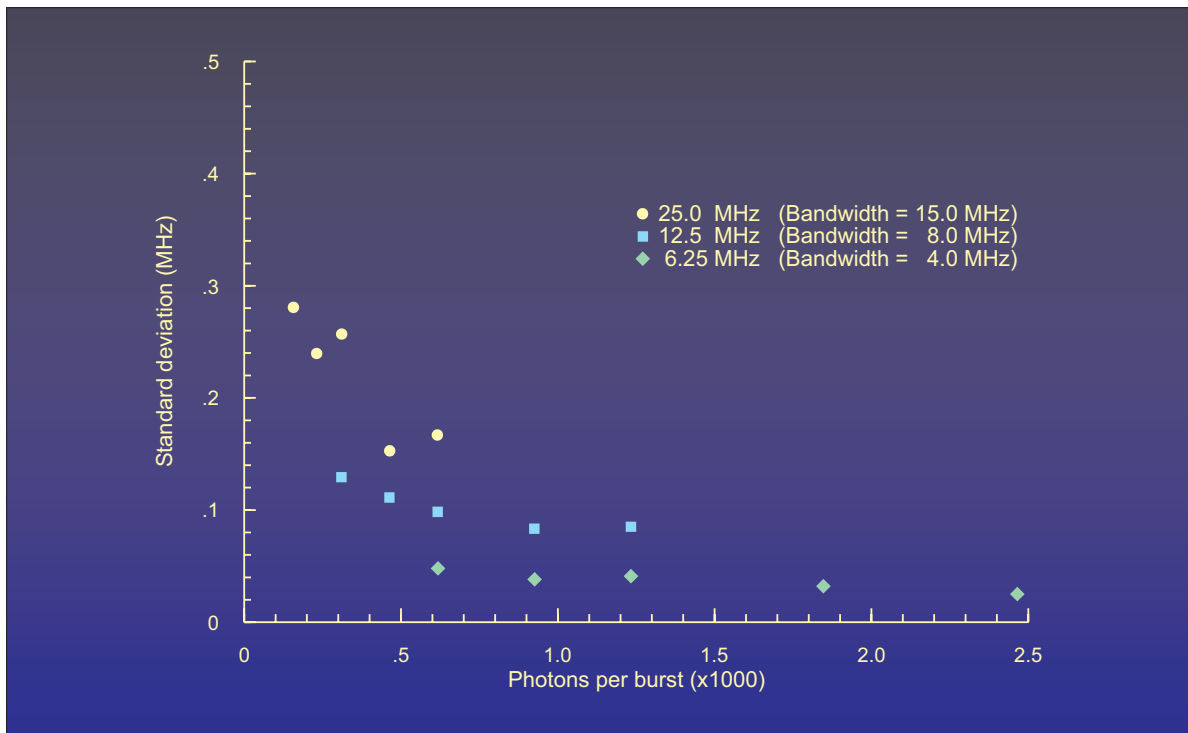


Figure 13. Effect of measurement uncertainty in the high-speed burst counter on standard deviation as a function of the number of photons contained within a signal burst.

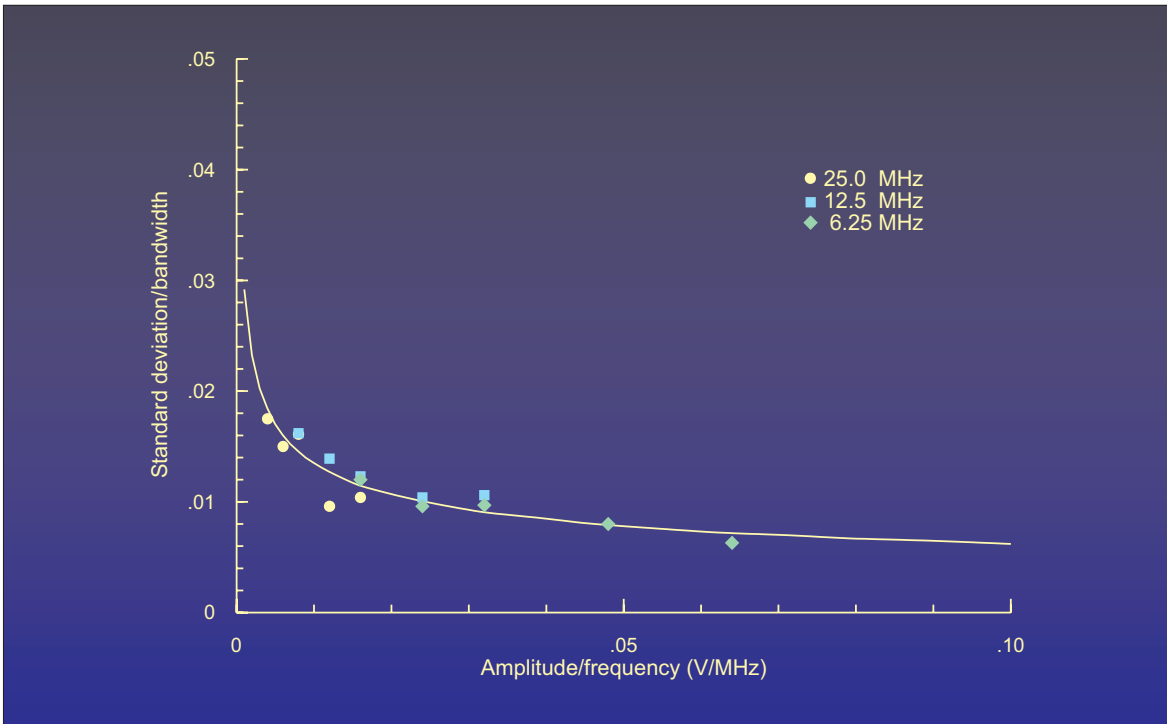


Figure 14. High-speed burst counter output standard deviation normalized by bandwidth as a function of input signal amplitude normalized by signal frequency.

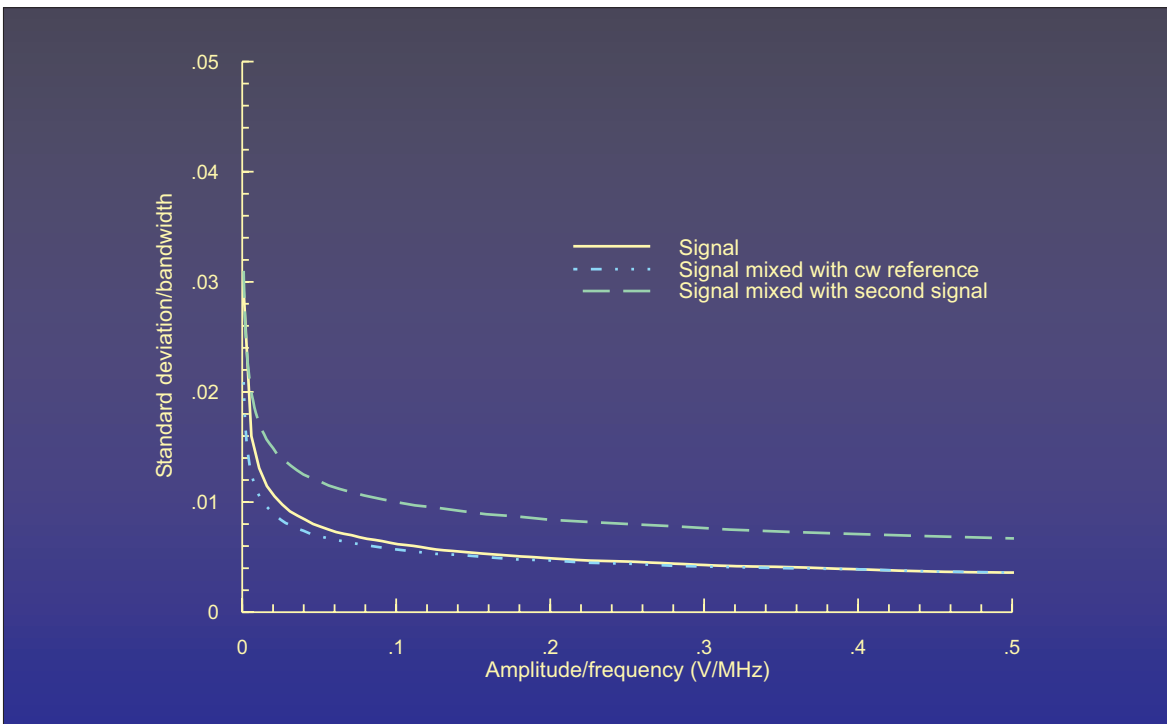


Figure 15. Predicted effect of electronic mixing on the high-speed burst counter output standard deviation normalized by bandwidth as a function of input signal amplitude normalized by signal frequency.